

We are IntechOpen, the world's leading publisher of Open Access books Built by scientists, for scientists

6,900

Open access books available

186,000

International authors and editors

200M

Downloads

Our authors are among the

154

Countries delivered to

TOP 1%

most cited scientists

12.2%

Contributors from top 500 universities



WEB OF SCIENCE™

Selection of our books indexed in the Book Citation Index
in Web of Science™ Core Collection (BKCI)

Interested in publishing with us?
Contact book.department@intechopen.com

Numbers displayed above are based on latest data collected.
For more information visit www.intechopen.com



An Evaluation of Severe Plastic Deformation on the Porosity Characteristics of Powder Metallurgy Aluminium Alloys Al-Mg-Si-Cu-Fe and Al-Zn-Mg-Cu

Róbert Bidulský¹, Marco Actis Grande¹

Jana Bidulská², Róbert Kočíško² and Tibor Kvačkaj²

¹*Politecnico di Torino – Sede di Alessandria*

²*Technical University of Košice, Faculty of Metallurgy*

Department of Metals Forming

¹*Italy*

²*Slovakia*

1. Introduction

Light weight aluminium alloys, showing excellent workability, high thermal and electrical conductivity, represent a good choice for the powder metallurgy (PM) industry to produce new materials having unique capabilities, not currently available in any other powder metal parts. Moreover the requirement on mechanical properties (i.e. high tensile strength with adequate plasticity) should assure an increasing role for aluminium alloys in the expanding PM market.

Room temperature tensile strengths in aluminium based metal matrix composites (MMC) in excess of 800 MPa have been reported (Guo & Kazama, 1997). However, PM based MMC currently show very limited application, also due to the high costs of production, thus having a low commercial appeal for both producers and end users. The application for aluminium powders is basically in the production of PM parts for structural and non-structural purposes in the transportation and commercial areas. Press and sinter products, blends of aluminium and elemental alloy powders are pressed into intricate configurations and sintered to yield net or near-net shapes. There are two interesting classes of commercial press and sinter aluminium alloys: Al-Mg-Si-Cu and Al-Zn-Mg-Cu-(Si). The first alloy displays moderate strength (the level of tensile strength is 240 MPa) while the latter alloy develops high mechanical properties (the level of tensile strength is 330 MPa) in both the as-sintered and heat-treated conditions. Solid solution strengthening and precipitation hardening can contribute to the higher strength values of the commercial alloys. (Pieczonka et al., 2008) report transverse strength of aluminium-based PM alloys in the range of 400 MPa (Al-Mg-Si-Cu) to 550 MPa (Al-Zn-Mg-Cu).

It's well known (Bidulská et al., 2008 a) that conventional forming methods and heat treatment can determine a limit in the level of strength-plastic characteristics adequate to structural properties. One possible way for achieving higher mechanical properties is

represented by severe plastic deformation (SPD), such as Equal Channel Angular Pressing (ECAP) (Valiev & Langdon, 2006); (Bidulská et al., 2008 b), (Kočiško et al., 2009); (Bidulská et al., 2010 a), as it is further confirmed in (Valiev et al., 2000), (Vinogradov et al., 2002). In the PM area, SPD is a relatively new technological solution for achieving high strength (Lapovok, 2005); (Wu et al., 2008); (Bidulská et al., 2010 b).

Al-Zn-Mg-Cu PM alloys, due to zinc show a poor sintering aid; these alloys do not have a good sintering response either. The high vapour pressure of zinc also gives rise to additional porosity, particularly when elemental powders are used (Lumley & Schaffer, 1998). Al-Zn-Mg-Cu PM alloys have been introduced as elemental powders or rich masteralloys (Neubing & Jangg, 1987); (Miura et al., 1993); (Danninger et al., 1998); (Neubing et al., 2002); (Gradl et al., 2004).

Solid state sintering of aluminium alloys has so far been unsuccessful, mainly due to the stable oxide layers on each particle. The main reason is the relative diffusion rates through the oxide and the aluminium alloys (Schaffer et al., 2001). Some activation is necessary to overcome this barrier and activate the sintering process by effective liquid phase sintering. An essential requirement for effective liquid phase sintering is a wetting liquid. Based on thermodynamically approach, magnesium reacts with aluminium oxide forming spinel, facilitating the disruption of oxide layer and thus wetting by liquid (Ziani & Pelletier, 1999); (Martín et al., 2002); (Martín & Castro, 2003). The reaction may be facilitated during sintering by diffusion of the magnesium through the aluminium matrix and will be accompanied by a change in volume, creating shear stresses in the film, ultimately leading to its break up. This is beneficial to the diffusion, wetting and therefore sintering. Several researches for a suitable design of various aluminium alloys for successful sintering (Martín et al., 2004); (Kim et al., 2004); (Rout et al., 2004); (Schaffer et al., 2001) have been developed. In particular, the effect of copper in the alloys seems to be efficacious and therefore the sintering behaviour of Al-Zn-Mg-Cu alloys needs to be developed properly. Authors (Kehl & Fischmeister, 1980) suggested that the Al-CuAl₂ eutectic can wet Al₂O₃ at 873 K. However, magnesium additions to molten aluminium reduce the contact angle sufficiently to produce wetting (Ip et al., 1993); (Liu et al., 1992). The work of adhesion of liquid metals on oxide surfaces increases with the free energy of formation of the metal oxide. It is therefore apparent that the oxide on aluminium is a barrier to sintering and needs to be overcome. Several works analyze the use of sintering additives on enhancing aluminium sinterability (Pieczonka et al., 2008); (Danninger et al., 1998), but few ones concentrated onto the evaluation of the role of porosity (Martín et al., 2004) on sintering behaviour and then on mechanical properties.

Most of the properties of PM materials are strongly related to porosity. Porosity can be used as an indicative parameter to evaluate and control the processes which the components underwent (Salak, 1997). The pores act as crack initiators and due to their presence distribution of stress is inhomogeneous across the cross section and leads to reduction of the effective load bearing area. Both the morphology and distribution of pores have a significant effect on the mechanical behaviour of PM materials. Two types of porosity are typically observed in sintered materials (Salak, 1997): interconnected and isolated porosity. Interconnected porosity has a more pronounced effect on properties than isolated porosity. The effect of porosity on the mechanical properties depends on the following factors (Pietrowski & Biallas, 1998); (Esper & Sonsino, 1994); (Marcu Puscas et al., 2003); (Bidulská et al., 2010 a); (Beiss & Dalgic, 2001):

- the quantity of pores (i.e., the fractional porosity) ;
- their interconnection;

- size;
- morphology;
- distribution;
- chemical composition;
- lubricant;
- die design and
- in terms of sintering:
- atmosphere,
- temperature and
- time.

In order to precisely evaluate the powder behaviour, new approaches are necessary (Hryha et al., 2009); (Mihalikova, 2010), as well as mathematical and computer simulation (Kim, 2002); (Bidulská et al., 2008 c); (Kvačakaj et al., 2007), mainly in the description of densification behaviour after SPD process.

In order to describe the dimensional and morphological porosity characteristics, the dimensional characteristic D_{circle} and the morphological characteristics f_{shape} and f_{circle} have been identified as the most effective parameters. The description of parameters is reported as follows:

- D_{circle} is the diameter of the equivalent circle that has the same area as the metallographic cross-section of the pore.
- f_{shape} and f_{circle} reflect the form of the pores.

The f_{shape} represents pore elongation, while f_{circle} depicts pore profile irregularity. Both parameters range between 0 and 1, being equal to unity for a circular pore. Elongation (elliptical deformation) as well as irregularity of the pore profile results in small values of f_{shape} and f_{circle} approaching 0 for highly elongated ones (Powder Metal Technologies and Applications, 1998); (DeHoff & Aigeltinger, 1970); (Marcu Puscas et al., 2003). Quantitative image analysis of investigated material treats pores as isolated plane two-dimensional objects in solid surroundings (Fig. 1).

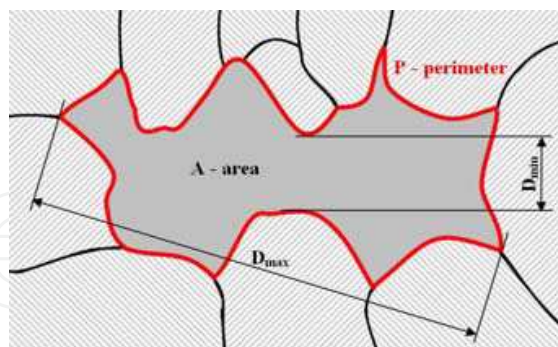


Fig. 1. The base characteristics by quantitative image analysis

The base characteristics are maximum and minimum pore dimensions D_{max} and D_{min} , pore area A , perimeter P and the diameter of the equivalent circle D_{circle} .

2. Experimental conditions

A commercial ready-to-press aluminium based powders (ECKA Alumix 321 and ECKA Alumix 431) were used as materials to be investigated. Formulations of the tested alloys are presented in Table 1 (wt. %).

Alumix 321					
Al	lubricant	Mg	Si	Cu	Fe
balance	1.50	0.95	0.49	0.21	0.07
Alumix 431					
Al	lubricant	Mg	Zn	Cu	-
balance	1.0	2.5	5.5	1.6	-

Table 1. Chemical compositions of investigated PM aluminium alloys

Particles size distribution, usually representing the mass percentage retained upon each of series of standard sieves of decreasing size and the percentage passed by the sieve of finest size, was carried out by sieve analyzer according to ISO 4497. The apparent density of powders was determined according to MPIF Standard 04. The tap density of powders was determined according to MPIF Standard 46. Specimens were obtained using a 2000 kN hydraulic press, applying different pressures. Unnotched impact energy specimens $55 \times 10 \times 10 \text{ mm}^3$ (ISO 5754) were prepared. The green compacts were weighed with an accuracy of $\pm 0.001 \text{ g}$. The dimensions were measured with a micrometer calliper ($\pm 0.01 \text{ mm}$). Specimens were dewaxed in a ventilated furnace (Nabertherm) at 673 K for 3600 s^{-1} . Sintering was carried out in a vacuum furnace (TAV) at 883 K for 1800 s^{-1} , with an applied cooling rate (post sintering) of 6 K/s . The cooling rate was monitored and recorded by means of thermocouples inserted in the central axis and close to the surface of the specimen. In vacuum furnaces, the cooling rate is generally determined by the pressure of the gas (N_2) introduced into the chamber. The SPD processes were divided to two separately steps, first step was ECAP-BP process and second was ECAP process. The set-up of ECAP-BP for the produced PM materials consisted of a vertical entrance channel with a forward pressing plunger and a horizontal exit channel with a back plunger providing a constant back pressure during pressing. The die had a 90° angle with sharp corners and channels of $6 \times 6 \text{ mm}^2$ in the cross section. Specimens were then inserted in the entrance channel with graphite lubrication. A heating device was employed to heat the die to 523 K , which was kept under control to $\pm 1 \text{ K}$ through a thermocouple mounted close to the intersection of the channels. A back pressure of 100 MPa was used. The specimens were ECAPed-BP for 1 pass. The ECAP was realized by hydraulic equipment at room temperature, which makes it possible to produce the maximum force of 1 MN . The die had a 90° angle with sharp corners and channels of diameter 10 mm in the cross section. The specimens were ECAPed for 1 pass.

Optical characterization was carried out on the minimum of 10 different image fields. For determination porosity characteristics were used magnification $100 \times$ for specimens prepared pressing and sintering and $500 \times$ for ECAPed specimens. Pores were recorded and processed by Leica Qwin image analysis system.

From these primary data a huge variety of secondary quantities can be derived which are used to describe pore size and pore shape. The scatter or deviations from primary data are mostly caused by delaminated specimens that were found in investigated aluminium alloys, mainly in low pressing pressure due to the low green strength or at very high pressing pressure due to the work hardening. The results in this investigation were sorted in number of processing pores in terms of processing conditions; for specimens prepared pressing and

sintering were processed a minimum of 1000 pores and for ECAPed specimens were processed a minimum of 300 pores.

The calculations of both morphological parameters are reported as follows:

$$f_{shape} = \frac{D_{min}}{D_{max}} = \frac{a}{b} \quad [-] \quad (1)$$

where:

D_{min} [μm], the parameter representing minimum of Feret diameter;

D_{max} [μm], the parameter representing maximum of Feret diameter;

and

$$f_{circle} = \frac{4 \cdot \pi \cdot A}{P^2} \quad [-] \quad (2)$$

where:

A [μm^2], the area of the metallographic cross-section of the pore, as the form

$$A = \pi \cdot a \cdot b \quad [\mu\text{m}^2] \quad (3)$$

P [μm], the perimeter of the metallographic cross-section of the pore, as the form

$$P = \pi [1.5 \cdot (a \cdot b) - \sqrt{a \cdot b}] \quad [\mu\text{m}] \quad (4)$$

3. Results and discussion

3.1 Effect of compacting pressure

The first stage of rigid die compaction is a basic forming technique used in the production of a lot of PM materials. It is primarily uniaxial compaction and the forming operation employs either a mechanical or a hydraulic press. A classical way for the evaluation of the powder compressibility is the relationship between the density or porosity and the applied pressure (Kawakita & Lüdde, 1971); (Panelli & Filho, 2001); (Hryha et al., 2008); (Denny, 2002); (Bidulská et al., 2009); (Bidulský et al., 2008). Different compacting pressures have been applied for the identification of the compressibility behaviour (100, 200, 300, 400, 500, 600 and 700 MPa) and the following compressibility equation (Dudrová et al., 1982); (Dudrová et al., 1983); (Parilák et al., 1983); (Parilák et al., 2004) was used:

$$P = P_0 \cdot \exp(-K \cdot p^n) \quad [\%] \quad (5)$$

where:

P [%], porosity achieved at an applied pressure p ;

P_0 [%], apparent porosity calculated from the value of experimentally estimated apparent density:

$$P_0 = \left[1 - \frac{\rho_a}{\rho_{th}} \cdot 100 \right] \quad [\%] \quad (6)$$

p [MPa], applied pressure;

K [-], a parameter related to particle morphology;

n [-], a parameter related to activity of powders to densification by the plastic deformation only.

Using the linear form of equation (5):

$$\ln \left[\ln \left(\frac{P_0}{P} \right) \right] = -\ln K + n \cdot \ln p \quad (7)$$

The parameters K and n can be calculated by linear regression analysis. A linear relationship between the parameters K and n was found and described in (Parilák et al., 2004):

$$\ln K = f(p): \quad \ln K = a - b \cdot n \quad (8)$$

where:

$a=1.432$;

$b=7.6$;

correlation coefficient $r=0.9665$.

The measured characteristics of the as-received aluminium powders are presented in Table 2 and Table 3, where the particle size distribution of both investigated aluminium alloys are reported. It can be seen from the results that the largest fraction of particles for the investigated material is in range of 63 to 100 μm . Particle size distribution of investigated aluminium alloys are presented in Table 2 and Table 3.

Size fraction [μm]	Fraction [%]	St. deviation
200-250	1.4	1.6
160-200	7.3	0.7
100-160	28.7	8.7
63-100	48.8	7.3
45-63	8.8	3.5
<45	5	5

Table 2. Particle size distribution of investigated Al-Mg-Si-Cu-Fe aluminium alloy

Size fraction [μm]	Fraction [%]	St. deviation
200-250	1	1.4
160-200	3.4	0.9
100-160	26.2	8.3
63-100	31.2	8.5
45-63	17.2	5.3
<45	21	7.1

Table 3. Particle size distribution of investigated Al-Zn-Mg-Cu aluminium alloy

Variations in particle size distribution and consequently the uniformity of powder mixes significantly influence the specimens' density and the mechanical properties including strength, wear and fatigue. Therefore, particle size distribution strongly affected apparent and tap density (Table 4). The finer Al-Zn-Mg-Cu alloy achieved 3 times higher tap density than Al-Mg-Si-Cu-Fe alloy. For example, the powders with a higher tap density generally have a lower sintered density than powders of similar size but different shape. The smaller the particles the greater the specific surface of the powder system is. (Powder Metal Technologies and Applications, 1998) suggested that this phenomenon increases the friction between particles and subsequently decreases the apparent density.

Table 4 reports the density properties of the studied systems.

No.	ρ_a [g.cm ⁻³]	ρ_t [g.cm ⁻³]	i [-]	ρ_{th} [g.cm ⁻³]
Al-Mg-Si-Cu-Fe	1.09	1.25	1.15	2.7134
Al-Zn-Mg-Cu	1.10	3.9	1.23	2.7213

Table 4. The fundamental density properties of investigated aluminium alloys

ρ_a is the apparent density, ρ_t is the tap density, i is the ratio ρ_{th} / ρ_a .

Table 5 shows the compressibility behaviour of the investigated systems.

No.	Po [%]	$K \cdot 10^{-2}$ [-]	n [-]	p_1 [MPa]	r [-]
Al-Mg-Si-Cu-Fe	59.83	1.57	0.4514	40.5	0.9934
Al-Zn-Mg-Cu	59.58	0.60	0.5822	106.2	0.9994

Table 5. Compressibility parameters of investigated aluminium alloys

p_1 represents the fictive pressure.

According to data listed in Table 5, the compressibility parameter n is related to the activity of powders to densification by the plastic deformation. In case of powders with high plasticity, n is close to 0.5; in case of low plasticity, n is close to 1. The results show excellent trends for both aluminium alloys. Al-Mg-Si-Cu-Fe alloy ($n = 0.4514$) shows a higher ability to plastically deform than Al-Zn-Mg-Cu alloy ($n = 0.5822$).

The effect of powder morphology also reflects in the values of the compressibility parameter K , which is lower for Al-Zn-Mg-Cu ($K = 0.60 \cdot 10^{-2}$) than for system Al-Mg-Si-Cu-Fe ($K = 1.57 \cdot 10^{-2}$). The difference between Al-Mg-Si-Cu-Fe and Al-Zn-Mg-Cu system is connected with the effect of particle geometry (represented by particle size distribution). It is very important to note that the lubrication of aluminium powder during compaction and ejection has to be considered since it has a strong tendency to stick to the tooling (Kehl et al., 1983); (Dudas & Dean, 1969); (Lefebvre et al., 2002).

Fig. 2 and Fig. 3 show the relationship between experimental and calculated data according to the aforementioned equations.

P_1 represents the "work" related to the densification done by particles transient rearrangement (for $n=1$). Compressibility of the Al-Mg-Si-Cu-Fe alloy is slightly higher than that of the Al-Zn-Mg-Cu alloy, mainly in the area of pressing pressures from 100 to 500 MPa.

The compressibility equation (5) enables to calculate the pressure p_1 needed for achieving almost close to zero porosity, only by particle movements. The results show a shifting from 106.2 MPa (Al-Zn-Mg-Cu) to 40.5 MPa for Al-Mg-Si-Cu-Fe.

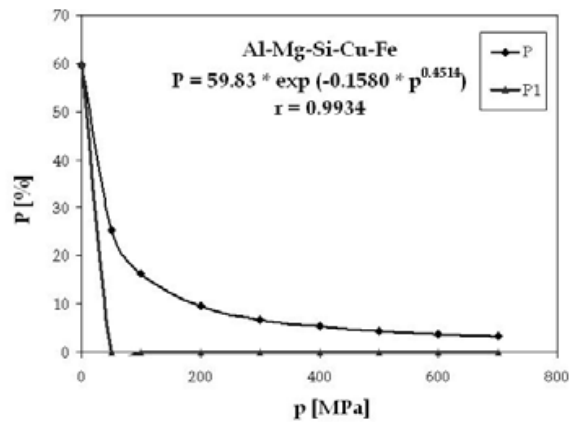


Fig. 2. Compressibility curves of Al-Mg-Si-Cu-Fe aluminium alloy

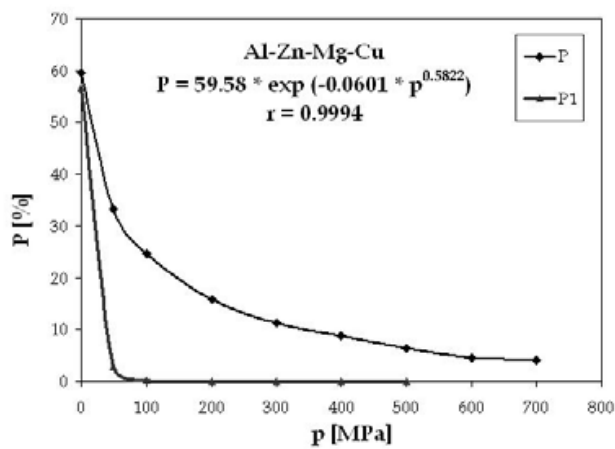


Fig. 3. Compressibility curves of Al-Zn-Mg-Cu alloy

The unetched microstructures after pressing are shown in the following figures.

Fig. 4 presents the typical microstructures for low pressures when the densification of the powder occurs by particle rearrangement (translations and rotations of particles) providing a higher packing coordination. Lower pressure creates high volume of porosity. Using low pressure may lead to edge blunting and porosity agglomeration, consequently a low green strength was found. It is clear visible, mainly in the microstructure of Al-Zn-Mg-Cu alloy.

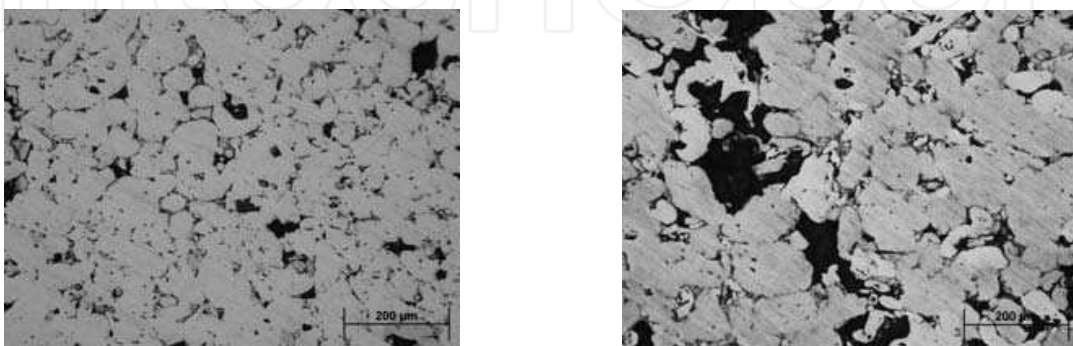


Fig. 4. Microstructure of aluminium alloys at 50 MPa, left - Al-Mg-Si-Cu-Fe, right - Al-Zn-Mg-Cu

After the finishing of particle rearrangement, the elastic and plastic deformation of particles starts through their contacts. Fig. 5 presents the detailed microstructures with small work hardened areas by implication of plastic deformation.

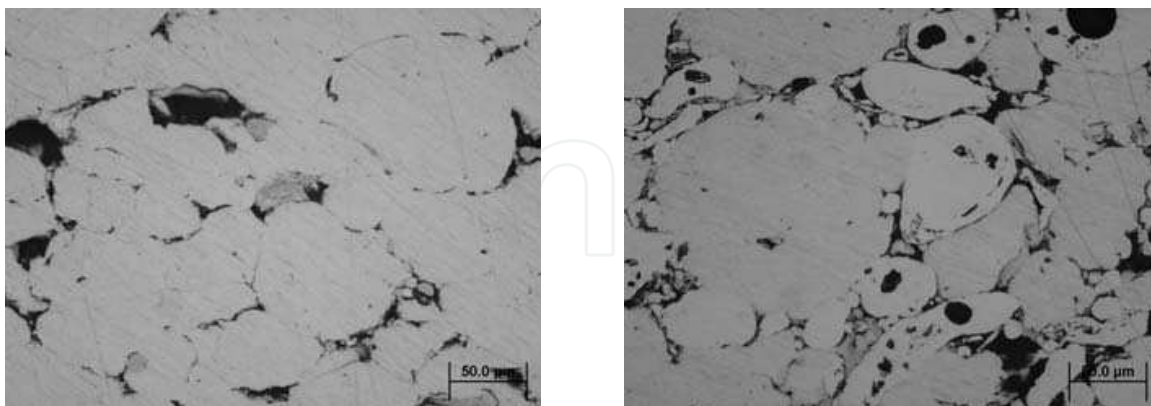


Fig. 5. Microstructure of aluminium alloys at 200 MPa, left - Al-Mg-Si-Cu-Fe, right - Al-Zn-Mg-Cu

Fig. 6 shows that the contact area between the particles increases and particles undergo extensive plastic deformation in both aluminium alloys. During compaction the particles deform following to the formation of solid interfaces at the point or planar particle contacts „*compaction facets*“ (Dudrová & Kabátová, 2007), representing areas with elevated free energy. Thus, the potential areas for nucleation and growth of inter-particle necks during the sintering are increased. In terms of compressibility, the pressing pressure of 400 MPa seems to be appropriate for achieving the desirable cold welding.

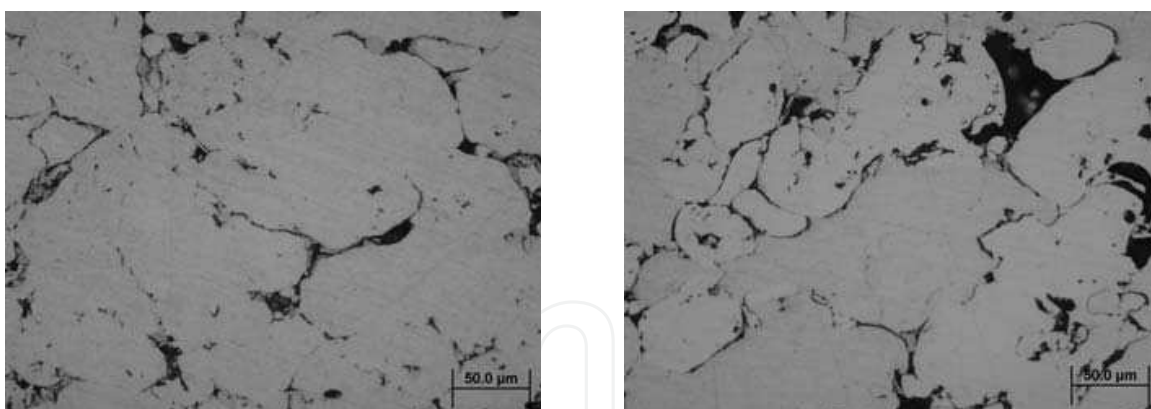


Fig. 6. Microstructure of aluminium alloys at 400 MPa, left - Al-Mg-Si-Cu-Fe, right - Al-Zn-Mg-Cu

The final stages of densification of powder particles under the pressure of 600 MPa are presented in Fig 7 (optical microscopy) and Fig. 8 (scanning electron microscopy).

In a number of materials densified by plastic flow, cusp-shaped pores <1 μm in size have been observed. The radius of material on the pore surface is much smaller than the particle radius. The material surrounding the pore has a shape typical of atomized produced powders (Fig. 9 right). Plastic deformation of powder particles leading to intimate contact between oxide- and/or contamination-free surfaces results in the formation of chemical bonds and adhesion, as confirmed by (Powder Metal Technologies and Applications, 1998).

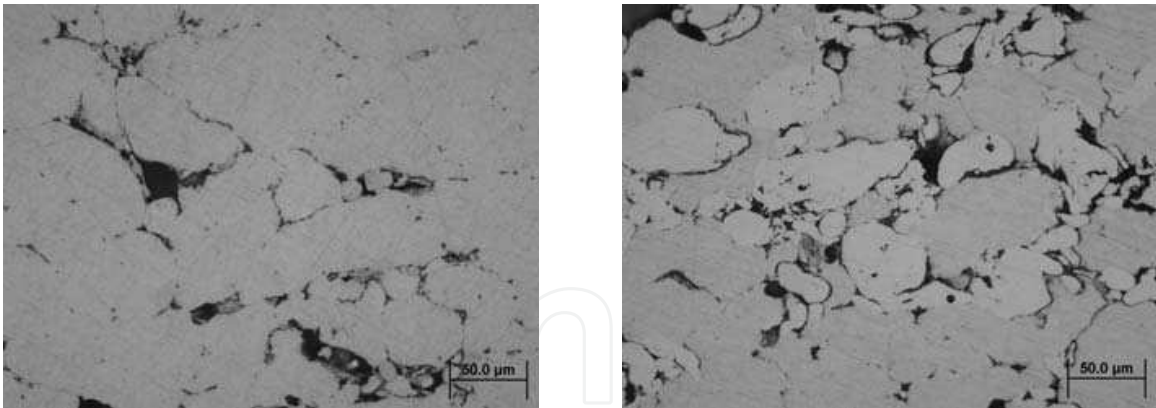


Fig. 7. Microstructure of aluminium alloys at 600 MPa, left - Al-Mg-Si-Cu-Fe, right - Al-Zn-Mg-Cu

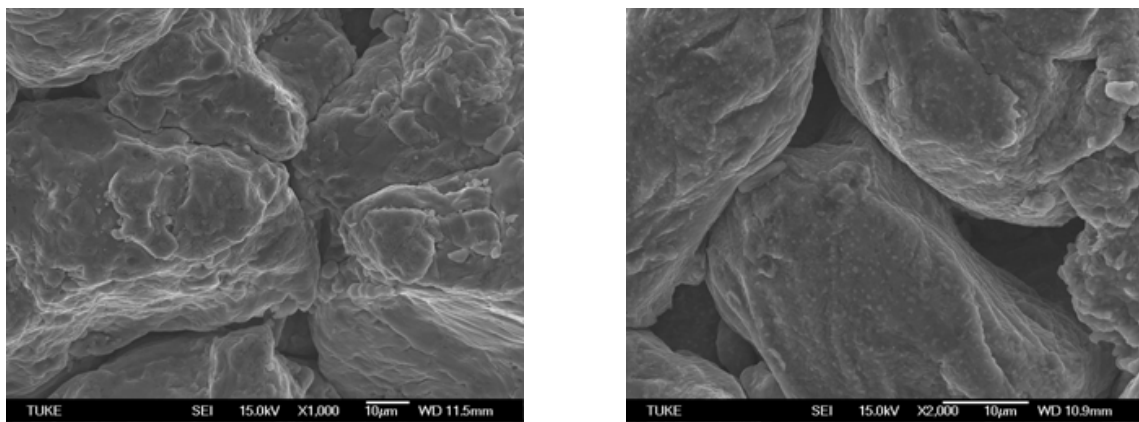


Fig. 8. Microstructure of aluminium alloys at 600 MPa, left - Al-Mg-Si-Cu-Fe, right - Al-Zn-Mg-Cu

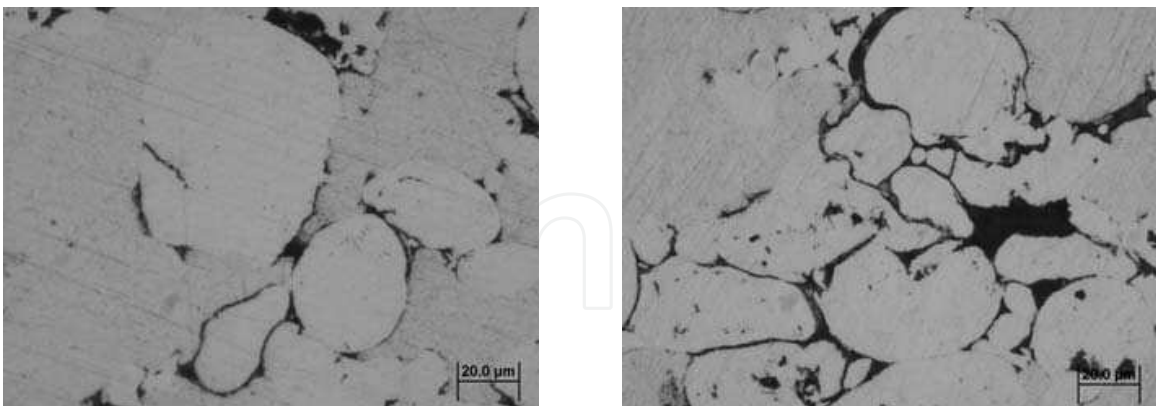


Fig. 9. Microstructure of aluminium alloys at 600 MPa, left, and 700 MPa, right - Al-Zn-Mg-Cu aluminium alloy

It is clear, that the Al-Mg-Si-Cu-Fe has a cold welding development bigger than the Al-Zn-Mg-Cu one. This is confirmed by the results of compressibility behaviour. The pore radius decreases with deformation. Such cusp-shaped pores are less stable under applied pressure than the spherical pores considered by (Powder Metal Technologies and Applications, 1998) formed by diffusional flow. What in principle opposes the closure of cusp-shaped pores is

the increasing surface tension force on the concave surfaces, resulting in LaPlace compressive stresses on these surfaces. At very high pressing pressure delaminated (cracking across the particle, Fig. 9) specimens were failing in the investigated systems; this is basically due to the work hardening effect.

3.2 Effect of sintering process

Consolidation of aluminium alloys by sintering presents a major problem: the oxide layer covering aluminium particles, Fig. 10.

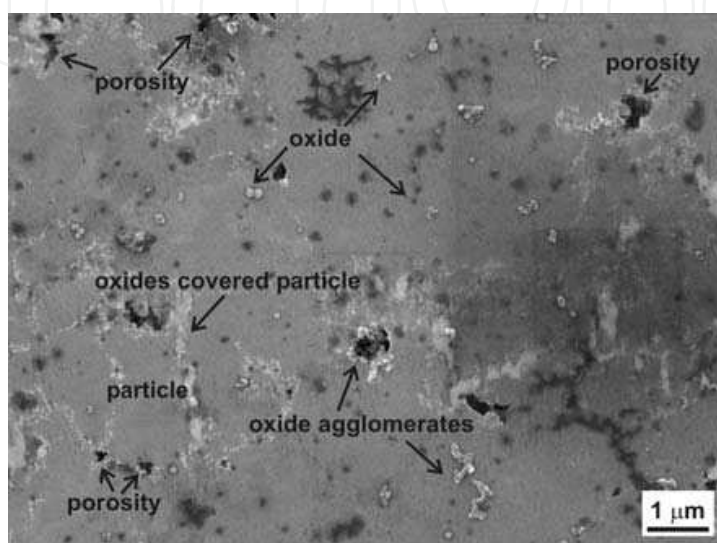


Fig. 10. Oxide layer covering aluminium particles

The oxide thickness is dependent on the temperature at which it is formed and the humidity contents in the atmosphere in which the powders is stored. Schaffer & Hall, 2002, suggested that the oxygen concentration in the nitrogen atmosphere is reduced by the aluminium through a self-gettering mechanism. The outer layers of the porous powder compact serve as a getter for the inner layers such that the oxygen partial pressure is reduced deep within the pore network. Aluminium nitride then forms, either by direct reaction with the metal or by reduction of the oxide layer, and sintering follows according to the equations.



It is highly exothermic: the $\Delta_f H_{AlN}^0 = -318 \text{ KJ/mol}$. If the temperature rises, as a consequence of the reaction, it will increase the liquid volume, which may enhance sintering (Schaffer et al., 2006). The oxide therefore prevents suitable bonding.

This has been explained in terms of the relative diffusion rates through the oxide and the metal, for metals with stable oxides. It means that, in order to achieve a good sintering response, aluminium alloys have to be modified by additional steps like, for example, severe plastic deformation or, in terms of pre-processing, master alloy powders. Liquid phase sintering of investigated aluminium alloys consists of typical stages. During the heating stage, the penetration of the pressing contacts by the transient liquid eutectic phases results in a pronounced expansion within a rather small temperature range. During further heating, when the solidus temperature for the composition is exceeded, also persistent liquid phase is formed, resulting in fast shrinkage. Depending on the selected heating rate and sintering

temperatures, the ratio solid-liquid varies and also the shrinkage does. The very sensitive solid-liquid equilibrium results in tight requirements for the tolerable temperature interval. It is well-known that for an effective liquid phase sintering, a wetting liquid represents an essential requirement. Authors (Kehl & Fischmeister, 1980) suggested that the Al-CuAl₂ eutectic can wet Al₂O₃ at 873 K. However, not even magnesium additions (to melt aluminium) reduce the contact angle sufficiently to produce wetting (Martín et al., 2004); (Danninger, 1987); (Martín & Castro, 2007). This is possibly the main reason why sintering Al-Zn-Mg-Cu and Al-Mg-Si-Cu-Fe aluminium alloys still cannot be considered that easy. It should be noticed that the investigated microstructures present the regions with alloying elements with high chemical activity, e.g. magnesium and copper, Figs. 11 and 12. Magnesium is mainly concentrated around the pores and in the necks volume. It appears that the primary porosity inside powder is also relatively permeable. The densification behaviour of powder particles in the examined alloy is complicated due to the large surface area and associated oxide layers. Formation of transient liquid phase, according to (Danninger & Gierl, 2001), enhances homogenization of the alloying element, mainly magnesium and copper, by accelerating material transport through spreading of the melt in the pore network and the pressing contacts and by increasing the diffusional cross-section.

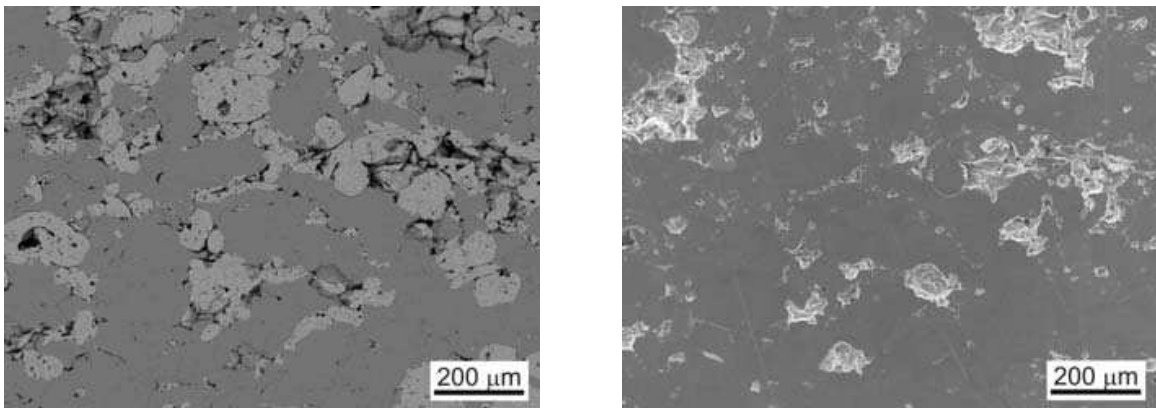


Fig. 11. The typical microstructure for 400 MPa pressed specimens, Al-Zn-Mg-Cu specimens, left SEI and right COMPO

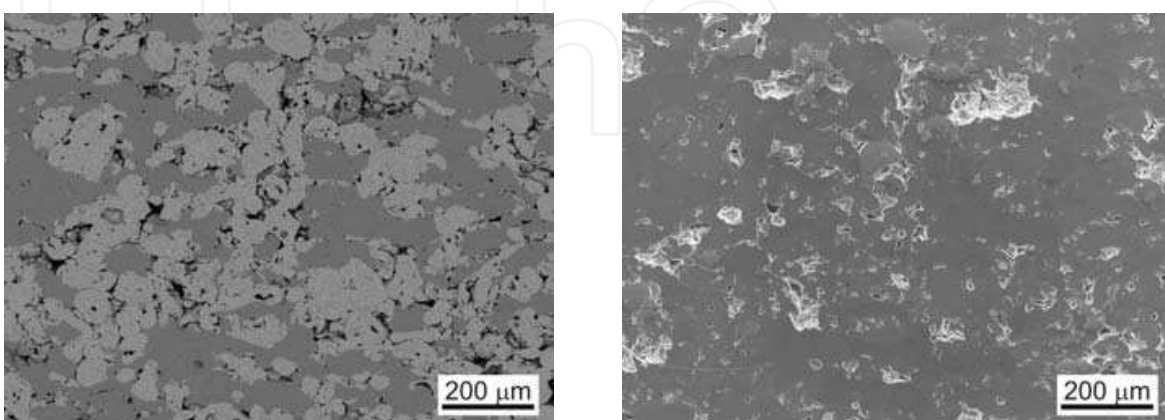


Fig. 12. The typical microstructure for 600 MPa pressed specimens, Al-Zn-Mg-Cu specimens, left SEI and right COMPO

Densification, Ψ , was calculated to determine the amount of shrinkage or swelling during sintering:

$$\Psi = \frac{\rho_s - \rho_g}{\rho_t - \rho_g} \quad [-] \quad (10)$$

where:

ρ_s [g.cm⁻³], the sintered density

ρ_g [g.cm⁻³], the green density and

ρ_{th} [g.cm⁻³], the theoretical density.

The results presented in Table 6 show values of theoretical density in different processing conditions as well as densification behaviour Ψ .

pressure [MPa]	pressing	dewaxing	sintering	Ψ	ECAP
400	92.48	93.11	92.12	-0.05	98.31
500	92.84	93.30	92.40	-0.06	98.39
600	93.03	92.89	92.82	-0.03	98.64
700	93.19	92.93	93.09	-0.01	98.58

Table 6. Densification behaviour of material as values of theoretical density (%), except Ψ (-).

Considering the first three columns, it can be seen that with increasing pressing pressure, the values of theoretical density increase. It is well-known that aluminium powder would not require much sintering because its relative softness allows very high green densities to be obtained by traditional uniaxial compaction alone; green densities in excess of 90% are typical. Indeed, sintering of aluminium often causes swelling and results in negative densification values (Lumley & Schaffer, 1998).

A high heating rate in transient systems also promotes liquid formation because it limits the time available for dissolution of the additive in the base prior to melting. ECAP process can be sufficient to achieve a good densification. Also, the presence of adsorbed and absorbed gases by the Al particles, as well as water vapour present during vacuum sintering (Showaiter & Youseffi, 2008) would increase the size of the compacts and therefore reducing their sintered density due to volume expansion.

As expected, the sintering brings to the formation of secondary porosity during transient LPS as well as the swelling presented seems to be related to the amount of liquid generated. The formation of secondary pores, according to (Martín et al., 2004); (Danninger, 1987); (Martín & Castro, 2007) is dependent to the previous formation of a liquid able to migrate away from the site of the prior alloying particles. The mix of primary (which still present in studied materials), secondary and residual porosity reveals the mean values of D_{circle} decreased with increasing pressing pressure. As expected, the coarse additive particle sizes leave large residual pores behind. Sintering under vacuum gave rise to the presence of higher pore content and excessive amounts of residual porosity at grain boundaries.

Table 7 shows the values of porosity characteristics for the investigated material processed before ECAP.

pressure [MPa]	D_{circle} [μm]	St. dev.	f_{shape} [μm]	f_{circle}
400	30.64	23.93	0.70	0.92
500	30.20	20.17	0.72	0.93
600	23.64	16.11	0.69	0.92
700	21.27	17.66	0.64	0.89

Table 7. Porosity distribution of studied material before ECAP

The successful densification of elemental powder mixtures by LPS is based on the formation of a combination of transient and permanent liquid phases (Martín et al., 2004); (Danninger, 1987). The LPS, firstly formed, allows the incorporation of alloying elements and therefore leads to swelling of the compacts. Another result of transient liquid phase is the presence of secondary pores. Since the melt spreads into the matrix pores and pressing contacts, it leaves pores behind, the diameter of which is correlated to the size of the original alloy particle.

The subsequently formed permanent liquid phases encourage densification accompanied by the corresponding shrinkage. On the other hand, this swelling-shrinkage sequence leads to distortion and to difficulties for dimensional control of the components.

The origin of compact swelling and the formation of secondary porosity during transient LPS are based on two main causes (Martín et al., 2004); (Schaffer et al., 2001). Firstly, the dissolution of the alloying particles in the metal matrix and secondly, the migration of a wetting liquid, formed from the alloying particles, through pore channels and/or the grain boundaries of the main component, Fig. 13. Both effects lead to the generation of secondary pores.

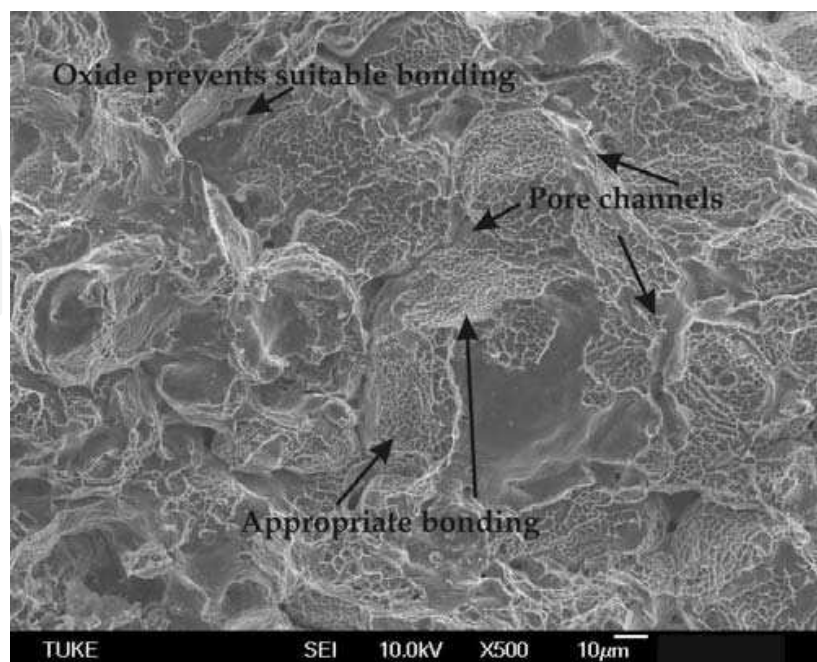


Fig. 13. Consolidation of aluminium alloys by sintering

3.3 Effect of SPD process

Effect of ECAP-BP

The processing way of ECAP-BP differs from ECAP in terms of the adopted temperature, which is settled at 523 K. The results of these investigations are presented in Table 8.

No. and pressure	D_{circle}	f_{shape}	f_{circle}
D, 400 MPa	10.47	0.53	0.25
D, 600 MPa	7.40	0.60	0.25
D+E, 400 MPa	5.75	0.59	0.27
D+E, 600 MPa	4.40	0.58	0.26
D+S+E, 400 MPa	3.18	0.46	0.22
D+S+E, 600 MPa	2.02	0.60	0.25

Table 8. Porosity distribution of studied material after ECAP-BP

Where: D-dewaxing, S-sintering, E-ECAP-BP

As expected, sintering coupled to back pressure tends to shift the distributions towards lower pores size D_{circle} and higher values of f_{shape} and f_{circle} since higher-temperature treatments leads to porosity reduction and improving pore morphology. Application of ECAP-BP supported next decreasing of pore size, represented by value of D_{circle} . It can be noted that most of the pores diameter values are in the range from 2 to 10 μm in all specimens, however rarely larger pores with the size up to 45 μm were observed.

It could be expected that this large amount of small pores strongly influences both f_{shape} and f_{circle} considering that small pores reveal preferably circular shape.

The results presented in Table 8 show a value of f_{circle} is in the range from 0.22 to 0.27. It is important to emphasize that f_{circle} depicts only how circular the form of the pore is, and f_{shape} include also how smooth the pore contour is, as it was shown in (Pavanati et al., 2007); the evolution of pores to a smooth contour is more effective than to a circular form during sintering, so the highest value of f_{shape} was registered for sintered and ECAPed specimen. Application of SPD process and sintering causes a decrease of D_{circle} to the minimum value of 2.02 and on the other hand, slightly increase the f_{circle} to maximum value of 0.27. It is interesting that, for both pressing pressure, the parameter D_{circle} has higher values for the initial state (after dewaxing) and the following processing (ECAP-BP and sintering plus ECAP-BP) causes contact areas between particles to increase and, consequently, a decrease in the effective shearing-stresses inside the particles. This condition happens with increasing densification, when the powder particles are plastically deformed and increasingly deformation strengthened. Dewaxing tends to generate larger pores in the microstructure, because of the lower densification attained on the green parts. When back pressure is applied, the stress distribution in deformed specimens causes the powder particles to squeeze together to such an extent that the initially interconnected pores transform to small semi-isolated pores, determining a lower value of parameter D_{circle} . Consequently, ECAP-BP influences the porosity distribution in terms of the severe shear deformation involving and therefore influences the pore morphology which is represented by both parameters of f_{shape} and f_{circle} .

Effect of ECAP

The application of ECAP supported the following decreasing of the pore size, represented by the value of D_{circle} , Table 9.

It can be noted that most of the pores diameter values are under 1 μm . It could be expected that this large amount of small pores (nanoporosity, Fig. 14), strongly influences both f_{shape} and f_{circle} considering that small pores evolve easily to a circular form despite of well-known ability of ECAP to alignment of particles (Lapovok, 2005); (Lapovok et al., 2008).

pressure [MPa]	D_{circle}	St. dev.	f_{shape}	f_{circle}
400	0.97	0.45	0.67	0.91
500	0.90	0.35	0.65	0.91
600	0.85	0.37	0.67	0.91
700	0.79	0.34	0.64	0.90

Table 9. Porosity distribution of studied material after ECAP

For the extremely large shear strains imposed by severe plastic deformation processing, even more extensive nucleation of nanopores is expected at grain boundaries or at particle-matrix interfaces (Lapovok et al., 2009). Formation of ultrafine grains during SPD processing increases the total area of grain boundaries and, therefore, the availability of nanopores nucleation sites. An additional effect of the continual grain refinement is an increase in the density of triple junctions that can act as preferred sites for nanopores nucleation. Lapovok et al. (2009) noted that small-angle X-ray scattering experiments on SPD-processed Al and an aluminium alloy carried out by (Betekhtin et al., 2007) provided useful insights in the effect of severe plastic deformation on formation of free volume, as also confirmed by (Divinski et al., 2009); (Ribbe et al., 2009), which was interpreted in terms of nanoporosity.

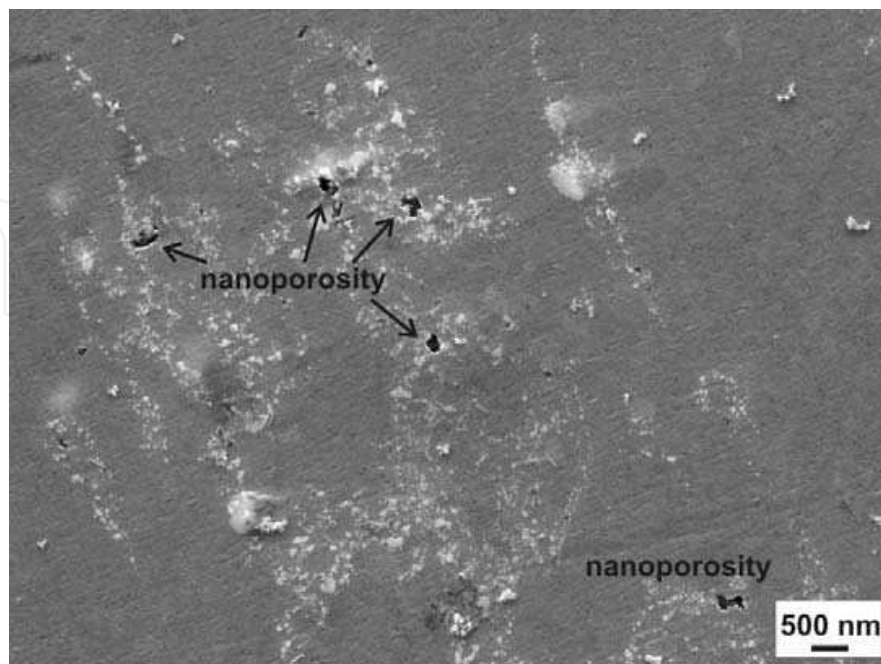


Fig. 14. Nanoporosity present in the studied material

Therefore, structure investigations by TEM (HRTEM) analysis will be useful key to identifications and confirmations the various theories about the material behaviour during the SPD processing (Dutkiewicz et al., 2009); (Lityńska-Dobrzyńska et al., 2010); (Maziarz et al., 2010); (Alexandrov et al., 2005).

4. Conclusion

In terms of compaction. The development of compressibility values with pressing pressure enables to characterize the effect of particles geometry and matrix plasticity on the compaction process. The presented results exhibit a high value of plasticity, as a property related to compressibility, and consequently promising compressibility data in terms of industrial potential applications are obtained.

In terms of sintering. The dissolution of the alloying particles in the metal matrix and therefore, the migration of a wetting liquid (formed from the alloying particles) through pore channels and/or the grain boundaries of the main component (promotes the swelling of compact) and the formation of secondary porosity, mainly at the prior alloying particle sites.

In terms of ECAP-BP. Analysis of presented parameters indicate that sintering coupled to SPD leads to porosity reduction and improving pore morphology. ECAP-BP influences the porosity distribution in terms of the severe shear deformation involved and therefore influences the pore morphology.

In terms of ECAP. The application of SPD, causing stress distribution in deformed specimens, made the powder particles to squeeze together to such an extent that the initially interconnected pores transform to small isolated pores, determining a given value of the parameter D_{circle} .

5. References

- Beiss, P. & Dalgic, M. (2001). Structure property relationships in porous sintered steels. *Materials Chemistry and Physics*, Vol. 67, (2001) 37-42, ISSN 0254-0584
- Bidulská, J.; Kvačkaj, T.; Bidulský, R. & Actis Grande M. (2008 a). Influence of processing conditions on EN AW 2014 material properties and fracture behavior. *Kovove Materialy*, Vol. 46, No. 6 (2008) 339-344, ISSN 0023-432X
- Bidulská, J.; Kvačkaj, T.; Bidulský, R. & Actis Grande M. (2008 b). Effect of Various Processing Conditions on the Tensile Properties and Structural Developments of EN AW 2014 Aluminium Alloy. *High Temperature Materials and Processes*, Vol. 27, No. 3 (2008) 203-207, ISSN 0334-6455
- Bidulská, J.; Kočiško, R.; Kvačkaj, T.; Bidulský, R. & Actis Grande, M. (2008 c). Numerical simulation of EN AW 2014 aluminium alloy in ECAP process. *Acta Metallurgica Slovaca*, Vol. 14, No. 3-4 (2008) 342-348, ISSN 1335-1532
- Bidulská, J. Kvačkaj, T. Actis Grande, M. & Bidulský, R. (2009). The compressibility behaviour of a new generation of coated metal/ceramic composite powders. *Key Engineering Materials*, Vol. 409 (2009) 362-364, ISSN 1013-9826
- Bidulská, J.; Kočiško, R.; Bidulský, R.; Actis Grande M.; Donič T. & Martikán M. (2010 a). Effect of severe plastic deformation on the porosity characteristics of Al-Zn-Mg-Cu PM alloy. *Acta Metallurgica Slovaca*, Vo. 16, No. 1 (2010) 4-11, ISSN 1335-1532

- Bidulská, J.; Kvačkaj, T.; Bidulský, R.; Actis Grande M.; Donič T. & Martikán M. (2010 b). Influence of ECAP-back pressure on the porosity distribution. *Acta Physica Polonica A*, Vol. 117, No. 5 (2010) 864-868, ISSN 0587-4246
- Bidulský, R. Actis Grande, M. Kabátová, M. & Selecká M. (2008). The effect of carbon coating and carbon admixing on the compressibility of Astaloy CrL. *Acta Metallurgica Slovaca*, Vol. 14, No. 3-4 (2008) 349-355, ISSN 1335-1532
- Betekhtin, V. I., Kadomtsev, A. G., Sklenicka, V. Saxl, I. (2007). Nanoporosity of fine-crystalline aluminum and an aluminum-based alloy. *Physics of the Solid State*, Vol. 49, No. 10 (2007) 1874-1877, ISSN 1063-7834
- Danninger, H. (1987). Secondary porosity in sintered steels and its effects on product quality and consistency. *Powder Metallurgy*, Vol. 30, No. 2 (1987) 103-109, ISSN 0032-5899
- Danninger, H.; Neubing, H. C. & Gradl, J. (1998). Sintering of High Strength Al-Zn-Mg-Cu Alloys to Controlled Dimensions. *Proceedings of Powder Metallurgy World Congress*, pp. 272-277, Vol. 5, Granada, 1998, EPMA, Shrewsbury
- Danninger, H. & Gierl, Ch. (2001). Processes in PM steel compacts during the initial stages of sintering. *Materials Chemistry and Physics*, Vol. 67 (2001) 49-55, ISSN 0254-0584
- DeHoff, R. T. & Aigeltinger, E. H. (1970). Experimental quantitative microscopy with special application to sintering. *Proceedings of Perspectives in Powder Metallurgy*, pp. 81-137, Vol.5, Plenum Press, New York
- Denny, P. J. (2002). Compaction equations: a comparison of the Heckel and Kawakita equations. *Powder Technology*, Vol. 127 (2002) 162-172, ISSN 0032-5910
- Divinski S. V., Ribbe J., Baither D., Schmitz G., Reglitz G., Rosner H., Sato K., Estrin Y., Wilde G. (2009). Nano- and micro-scale free volume in ultrafine grained Cu-1 wt.%Pb alloy deformed by equal channel angular pressing. *Acta Materialia*, Vol. 57, No. 19 (2009) 5706-5717, ISSN: 1359-6454
- Dudas, J. H. & Dean, W. A. (1969). The production of precision aluminum P/M parts. *International Journal of Powder Metallurgy*, Vol. 5, No. 2 (1969) 21-36, ISSN 0888-7462.
- Dudrová, E. Parilák, L. Rudnayová, E. & Šlesár, M. (1982). Physico-metallurgical principles of compaction, sintering and their relation with the properties of porous materials. *Proceedings of 6th International Conference on Powder Metallurgy in ČSSR*, pp. 73-83, Part 1, Brno, 1982, DT ČSVTS, Žilina
- Dudrová, E. Rudnayová, E. & Parilák, L. (1983). Lisovanie práškových kovov. *Pokroky práškové metalurgie*, Vol. 21, No. 2 (1983) 29-50, ISSN 0322-9769
- Dudrová, E. & Kabátová, M. (2007). Microstructural Defects and Properties. *Proceedings of Design and Capabilities of PM Components and Materials. A Residential Training Course for Young Materials/Design Engineers*. pp. 513-535, Vol. 2. Košice, 23.6.-1.7.2007, EPMA
- Dutkiewicz, J.; Masdeu, F.; Malczewski, P. & Kukuła, A. (2009). Microstructure and properties of $\alpha + \beta$ brass after ECAP processing. *Archives of Materials Science and Engineering*, Vol. 39, No. 2 (2009) 80-83, ISSN 1897-2764
- Esper, F. J. & Sonsino, C. M. (1994). *Fatigue design for PM components: Manual for Design and Production Engineers*, EPMA, ISBN 1-899072-00-4, Shrewsbury

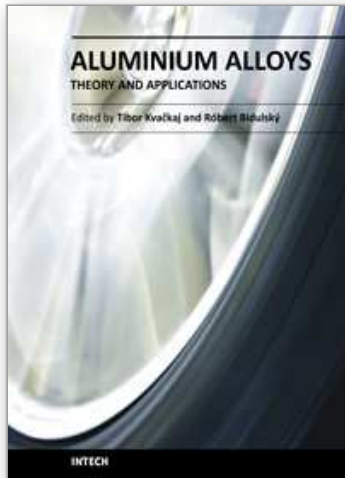
- Gradl, J.; Neubing, H. C. & Müller, A. (2004). Improvement in the Sinterability of 7-xxx-based Aluminium Premix. *Proceedings of Euro Powder Metallurgy*, pp. 15-21, Vol. 4, Eds. Danninger, H. & Ratzi, R., Wien, 2004, EPMA, Shrewsbury
- Guo, J.Q. & Kazama, N.S. (1997). Mechanical properties of rapidly solidified Al-Ti-Fe, Al-Cu-Fe and Al-Fe-Cu-Ti based alloys extruded from their atomized powders. *Materials Science and Engineering A*, Vol. 232, No. 1-2 (1997) 177-182, ISSN 0921-5093
- Hryha, E. Dudrová, E. & Bengtsson, S. (2008). Influence of powder properties on compressibility of prealloyed atomised powders. *Powder Metallurgy*, Vol. 51, No. 4 (2008) 340-342, ISSN 0032-5899
- Hryha, E.; Zubko, P.; Dudrová, E.; Pešek, L. & Bengtsson, S. (2009). An application of universal hardness test to metal powder particles. *Journal of Materials Processing Technology*, Vol. 209, No. 5 (2009) 2377-2385, ISSN 0924-0136
- Ip, S. W.; Kucharski, M. & Toguri, J. M. (1993). Wetting behaviour of aluminium and aluminium alloys on Al₂O₃ and CaO. *Journal of Materials Science Letters*, Vol. 12, No. 21 (1993) 1699-1702, ISSN 0261-8028
- Kawakita, J. & Lüdde, K. H. (1971). Some considerations on powder compression equation. *Powder Technology*, Vol. 4, No. 2 (1971) 61-68, ISSN 0032-5910
- Kehl, W. & Fischmeister H. F. (1980). Liquid-phase sintering of Al-Cu compacts. *Powder Metallurgy*, Vol. 23, No. 3 (1980) 113-119, ISSN 0032-5899
- Kehl, W.; Bugajska, M. & Fischmeister, H. F. (1983). Internal or die wall lubrication for compaction of Al powders. *Powder Metallurgy*, Vol. 26, No. 4 (1983) 221-227, ISSN 0032-5899
- Kim, H. S. (2002). Finite element analysis of deformation behaviour of metals during equal channel multi-angular pressing. *Materials Science and Engineering A*, Vol. 328, No. 1-2 (2002) 317-323, ISSN 0921-5093
- Kim, Y. D.; Min, K. H.; Kang, S. P. & Chang, S.-Y. (2004). PM Lightweight and Porous Materials Effect of Mg Addition on Sintering Characteristic of 7xxx Series Al P/M Alloy. *Proceedings of Euro Powder Metallurgy*, pp. 40-45, Vol. 4, Eds. Danninger, H. & Ratzi, R., Wien, 2004, EPMA, Shrewsbury
- Kočíško, R.; Kvačkaj, T.; Bidulská, J. & Molnárová M. (2009). New Geometry of ECAP Channels. *Acta Metallurgica Slovaca*, Vol. 15, No. 4 (2009) 228-233, ISSN 1335-1532
- Kvačkaj, T.; Zemko, M.; Kočíško, R.; Kuskulič, T.; Pokorny, I.; Besterci, M.; Sulleiova, K.; Molnarova, M.; Kovačova, A. (2007). Simulation of ECAP process by finite element method. *Kovove Materialy*, Vol. 45, No. 5 (2007) 249-25, ISSN 0023-432X
- Lapovok, R.Y. (2005). The role of back-pressure in equal channel angular extrusion. *Journal of Materials Science*, Vol. 40, No. 2 (2005) 341-346, ISSN 0022-2461
- Lapovok, R. Y.; Tomus, D. & Muddle B. C. (2008). Low-temperature compaction of Ti-6Al-4V powder using equal channel angular extrusion with back pressure. *Materials Science and Engineering A*, Vol. 490, No. 1-2 (2008) 171-180, ISSN 0921-5093
- Lefebvre, L.-P.; Thomas, Y. & White, B. (2002). Effects of lubricants and compacting pressure on the processability and properties of aluminum P/M parts. *Journal of Light Metals*, Vol. 2, No. 4 (2002) 239-246, ISSN 1471-5317

- Lityńska-Dobrzyńska, L.; Dutkiewicz, J.; Maziarz, W. & Rogal, I. (2010). TEM and HRTEM studies of ball milled 6061 aluminium alloy powder with Zr addition. *Journal of Microscopy*, Vol. 237, No. 3 (2010) 506-510, ISSN 0022-2720
- Liu, Y.; He, Z.; Dong, G. & Li, Q. (1992). The effect of cerium on the wettability of Al₂O₃/Al-4.5Cu alloy. *Journal of Materials Science Letters*, Vol. 11, No. 12 (1992) 896-898, ISSN 0261-8028
- Lumley, R.N. & Schaffer, G.B. (1998). Precipitation induced densification in a sintered Al-Zn-Mg-Cu alloy. *Scripta Materialia*, Vol. 39, No. 8 (1998) 1089-1094, ISSN 1359-6462
- Lumley, R. N. Sercombe, T. B. & Schaffer, G. B. (1999). Surface oxide and the role of magnesium during the sintering of aluminum. *Metallurgical and Materials Transactions A*, Vol. 30, No. 2 (1999) 457-463, ISSN 1073-5623
- Marcu Puscas, T.; Signorini, M.; Molinari, A. & Straffelini, G. (2003). Image analysis investigation of the effect of the process variables on the porosity of sintered chromium steels. *Materials Characterization*, Vol. 50, No. 1 (2003) 1-10, ISSN 1044-5803
- Martín, J. M.; Gómez-Acebo, T. & Castro, F. (2002). Sintering behaviour and mechanical properties of PM Al-Zn-Mg-Cu alloy containing elemental Mg additions. *Powder Metallurgy*, Vol. 45, No. 2 (2002) 173-180, ISSN 0032-5899
- Martín, J. M. & Castro, F. (2003). Alloy development and associated dimensional changes of aluminium alloys during liquid phase sintering. *Materials Science Forum*, Vol. 426-432 (2003) 107-114, ISSN 0255-5476
- Martín, J. M.; Navarcorena, B.; Arribas, I.; Gómez-Acebo, T. & Castro, F. (2004). *Dimensional Changes and Secondary Porosity in Liquid Phase Sintered Al Alloys*, *Proceedings of Euro Powder Metallurgy*, pp. 46-53, Vol. 4, Eds. Danninger, H. & Ratzi, R., Wien, 2004, EPMA, Shrewsbury
- Martín, J.M. & Castro, F. (2007). Sintering response & microstructural evolution of an Al-Cu-Mg-Si premix. *International Journal of Powder Metallurgy*, Vol. 43, No. 6 (2007) 59-69, ISSN 0888-7462
- Maziarz, W.; Dutkiewicz, J.; Lityńska-Dobrzyńska, L.; Santamarta, R. & Cesari, E. (2010). Structure investigations of ferromagnetic Co-Ni-Al alloys obtained by powder metallurgy. *Journal of Microscopy*, Vol. 237, No. 3 (2010) 374-378, ISSN 0022-2720
- Mihalikova, M. (2010). Research of strain distribution and strain rate change in the fracture surroundings by the videoextensometric method. *Metalurgija*, Vol. 49, No. 3 (2010) 161-164, ISSN 0543-5846
- Miura, S.; Machida, Y.; Hirose, Y. & Yoshimura, R. (1993). The Effects of Varied Alloying Methods on the Properties of Sintered Aluminum Alloys. *Proceedings of Powder Metallurgy World Congress*, pp. 571-574, Japan, 1993, Kyoto, JSPPM
- Neubing, H. C. & Jangg, G. (1987). Sintering of aluminum parts: the state-of-the-art. *Metal Powder Report*, Vol. 42, No. 5 (1987) 354-358, ISSN 0026-0657
- Neubing, H. C.; Gradl J. & Danninger H. (2002). Sintering and Microstructure of Al-Si PM Components. *Proceedings of Advances in Powder Metallurgy & Particulate Materials*, pp. 128-138, Part 13, Eds. Arnhold, V.; Chu, Ch.-L.; Jandeska, W. F. & Sanderow, H. I., 2002, MPIF, Orlando

- Parilák, L. Dudrová, E. & Rudnayová, E. (1983). Aproximativne vyjadrenie lisovacej krivky technických práškových kovov. *Pokroky práškové metalurgie*, Vol. 21, No. 3 (1983) 19-30, ISSN 0322-9769
- Parilák, L. Dudrová, E. Bidulský, R. & Kabátová, M. (2004). Quantification of metal powder compressibility in uniaxial compaction. *Proceedings of Euro Powder Metallurgy*, pp. 593-598, Vol. 4, Eds. Danninger, H. & Ratzi, R., Wien, 2004, EPMA, Shrewsbury
- Panelli, R. & Filho, F. A. (2001). A study of a new phenomenological compacting equation. *Powder Technology*, Vol. 114, No. 1 (2001) 255-261, ISSN 0032-5910
- Pavanati, H. C.; Maliska, A. M.; Klein, A. N. & Muzart, J. L. R. (2007). Comparative study of porosity and pores morphology of unalloyed iron sintered in furnace and plasma reactor. *Materials Research*, Vol. 10, No. 1 (2007) 87-93, ISSN 1516-1439
- Pieczonka, T.; Schubert, Th.; Baunack, S. & Kieback B. (2008). Dimensional behaviour of aluminium sintered in different atmospheres. *Materials Science and Engineering A*, Vol. 478, No. 1-2 (2008) 251-256, ISSN 0921-5093
- Pietrowski, A. & Biallas, G. (1998). Influence of sintering temperature on pore morphology, microstructure, and fatigue behaviour of MoNiCu alloyed sintered steel. *Powder Metallurgy*, Vol. 41, No. 2 (1998) 109-114, ISSN 0032-5899
- Powder Metal Technologies and Applications (1998). Vol. 7, ASM Handbook, ISBN 0-87170-387-4, First printing, December 1998, ASM International, Warrendale
- Ribbe, J., Baither D., Schmitz G., Divinski S. V. (2009). Network of Porosity Formed in Ultrafine-Grained Copper Produced by Equal Channel Angular Pressing. *Physical Review Letters*, Vol.102, No. 16 (2009) 165501, ISSN 0031-9007
- Rout, S. K.; Veltl, G. & Petzoldt, F. (2004). Effect of Sn additions on Microstructure Evolution in Sintered Aluminium Alloys. *Proceedings of Euro Powder Metallurgy*, pp. 9-14, Vol. 4, Eds. Danninger, H. & Ratzi, R., Wien, 2004, EPMA, Shrewsbury
- Salak, A. (1997). *Ferrous Powder Metalurgy*. Cambridge International Science Publishing, ISBN-13: 978-1-898326-03-7, Cambridge
- Schaffer, G.B.; Sercombe, T.B. & Lumley, R.N. (2001). Liquid phase sintering of aluminium alloys. *Materials Chemistry and Physics*, Vol. 67, No. 1-3 (2001) 85-91, ISSN 0254-0584
- Schaffer, G.B. & Hall, B. J. (2002). The influence of the atmosphere on the sintering of aluminum. *Metallurgical and Materials Transactions A*, Vol. 33, No. 10 (2002) 3279-3284, ISSN 1073-5623
- Schaffer, G. B.; Hall, B. J.; Bonner, S. J.; Huo, S. H. & Sercombe, T. B. (2006). The effect of the atmosphere and the role of pore filling on the sintering of aluminium. *Acta Materialia*, Vol. 54 (2006) 131-138, ISSN 1359-6454
- Showaiter, N. & Youseffi, M. (2008). Compaction, sintering and mechanical properties of elemental 6061 Al powder with and without sintering aids. *Materials and Design*, Vol. 29, No. 4 (2008), 752-762, ISSN 0261-3069
- Valiev, R.Z. , Islamgaliev, R.K. & Alexandrov I.V. (2000). Bulk nanostructured materials from severe plastic deformation. *Progress in Materials Science*, Vol. 45, No. 2 (2000) 103-189, ISSN 0079-6425
- Valiev, R.Z. & Langdon, T.G. (2006). Principles of equal-channel angular pressing as a processing tool for grain refinement. *Progress in Materials Science*, Vol. 51, No. 7 (2006) 881-981, ISSN 0079-6425

- Vinogradov, A.; Patlan, V. ; Suzuki, Y.; Kitagawa K. & Kopylov, V.I. (2002). Structure and properties of ultra-fine grain Cu-Cr-Zr alloy produced by equal-channel angular pressing. *Acta Materialia*, Vol. 50, No. 7 (2002) 1636-1651, ISSN 1359-6454
- Ziani, A. & Pelletier, S. (1999). Supersolidus liquid-phase sintering behavior of degassed 6061 Al powder. *International Journal of Powder Metallurgy*, Vol 35, No. 8 (1999) 49-58, ISSN 0888-7462
- Wu, X.; Xu, W. & Xia K. (2008). Pure aluminum with different grain size distributions by consolidation of particles using equal-channel angular pressing with back pressure. *Materials Science and Engineering A*, Vol. 493, No. 1-2 (2008) 241-245, ISSN 0921-5093

IntechOpen



Aluminium Alloys, Theory and Applications

Edited by Prof. Tibor Kvackaj

ISBN 978-953-307-244-9

Hard cover, 400 pages

Publisher InTech

Published online 04, February, 2011

Published in print edition February, 2011

The present book enhances in detail the scope and objective of various developmental activities of the aluminium alloys. A lot of research on aluminium alloys has been performed. Currently, the research efforts are connected to the relatively new methods and processes. We hope that people new to the aluminium alloys investigation will find this book to be of assistance for the industry and university fields enabling them to keep up-to-date with the latest developments in aluminium alloys research.

How to reference

In order to correctly reference this scholarly work, feel free to copy and paste the following:

Róbert Bidulský, Marco Actis Grande, Jana Bidulská, Róbert Kočiško and Tibor Kvačkaj (2011). An Evaluation of Severe Plastic Deformation on the Densification Behaviour of Powder Metallurgy Aluminium Alloy Al-Mg-Si-Cu-Fe and Al-Zn-Mg-Cu, *Aluminium Alloys, Theory and Applications*, Prof. Tibor Kvackaj (Ed.), ISBN: 978-953-307-244-9, InTech, Available from: <http://www.intechopen.com/books/aluminium-alloys-theory-and-applications/an-evaluation-of-severe-plastic-deformation-on-the-densification-behaviour-of-powder-metallurgy-alum>

INTECH

open science | open minds

InTech Europe

University Campus STeP Ri
Slavka Krautzeka 83/A
51000 Rijeka, Croatia
Phone: +385 (51) 770 447
Fax: +385 (51) 686 166
www.intechopen.com

InTech China

Unit 405, Office Block, Hotel Equatorial Shanghai
No.65, Yan An Road (West), Shanghai, 200040, China
中国上海市延安西路65号上海国际贵都大饭店办公楼405单元
Phone: +86-21-62489820
Fax: +86-21-62489821

© 2011 The Author(s). Licensee IntechOpen. This chapter is distributed under the terms of the [Creative Commons Attribution-NonCommercial-ShareAlike-3.0 License](#), which permits use, distribution and reproduction for non-commercial purposes, provided the original is properly cited and derivative works building on this content are distributed under the same license.

IntechOpen

IntechOpen